Time-dependent density functional theory study on the electronic excited-state hydrogen bonding of the chromophore coumarin 153 in a room-temperature ionic liquid

ARTICLE *in* JOURNAL OF MOLECULAR MODELING · JUNE 2011

Impact Factor: 1.74 · DOI: 10.1007/s00894-011-1131-3 · Source: PubMed

5 AUTHORS, INCLUDING:

Dandan Wang
Dalian University of Technology
6 PUBLICATIONS **18** CITATIONS
SEE PROFILE

Ce Hao
Dalian University of Technology
134 PUBLICATIONS **916** CITATIONS
SEE PROFILE

Jie Shan Qiu
Dalian University of Technology
421 PUBLICATIONS **7,173** CITATIONS
SEE PROFILE

J Mol Model
DOI 10.1007/s00894-011-1131-3

ORIGINAL PAPER

Time-dependent density functional theory study on the electronic excited-state hydrogen bonding of the chromophore coumarin 153 in a room-temperature ionic liquid

Dandan Wang · Ce Hao · Se Wang · Hong Dong · Jieshan Qiu

Received: 7 February 2011 / Accepted: 15 May 2011

Abstract In the present work, in order to investigate the electronic excited-state intermolecular hydrogen bonding between the chromophore coumarin 153 (C153) and the room-temperature ionic liquid *N*,*N*-dimethylethanolammonium formate (DAF), both the geometric structures and the infrared spectra of the hydrogen-bonded complex C153–DAF^+ in the excited state were studied by a time-dependent density functional theory (TDDFT) method. We theoretically demonstrated that the intermolecular hydrogen bond $C_1{=}O_1{\cdots}H_1{-}O_3$ in the hydrogen-bonded C153–DAF^+ complex is significantly strengthened in the S_1 state by monitoring the spectral shifts of the C=O group and O–H group involved in the hydrogen bond $C_1{=}O_1{\cdots}H_1{-}O_3$. Moreover, the length of the hydrogen bond $C_1{=}O_1{\cdots}H_1{-}O_3$ between the oxygen atom and hydrogen atom decreased from 1.693 Å to 1.633 Å upon photoexcitation. This was also confirmed by the increase in the hydrogen-bond binding energy from 69.92 kJ mol^{-1} in the ground state to 90.17 kJ mol^{-1} in the excited state. Thus, the excited-state hydrogen-bond strengthening of the coumarin chromophore in an ionic liquid has been demonstrated theoretically for the first time.

Keywords Hydrogen-bonding dynamics · Excited state · Hydrogen bond strengthening · Spectral shift

D. Wang · C. Hao (✉) · S. Wang · H. Dong · J. Qiu
State Key Laboratory of Fine Chemicals,
School of Chemical Engineering,
Dalian University of Technology,
Dalian,
116024 Liaoning, China
e-mail: haoce_dlut@126.com

Introduction

Numerous experimental and theoretical methods have been developed to investigate the nature of a hydrogen bond linking a solute with a polarizable functional group and a protic solvent. Since intermolecular hydrogen bonds are site-specific solute–solvent interactions, they play a fundamental role in the molecular photochemistry of organic and biological chromophores in solution [1–24]. Upon photoexcitation, the intermolecular hydrogen bonds formed between solute and solvent molecules will reorganize themselves as the result of differences in the charge distribution of the different electronic states; this process is termed *hydrogen-bonding dynamics*, and it is linked to photochemical and photophysical processes [25–31]. A strengthening of the hydrogen bond between C102 and phenol early during photoexcitation to the electronic excited state was first demonstrated by Zhao and Han theoretically [4], and since then a great deal of work has focused on hydrogen-bonding dynamics in the excited state [4–10]. Their work has already yielded much information on the structural and relaxation dynamics of hydrogen bonds after photoexcitation, which has aided our understanding of fluorescence-quenching phenomena in the excited state [32–35]. However, previous studies focused on the intermolecular hydrogen bonds that form between chromophores and traditional polar protic solvents, and while great progress has been made in this field [36–44], fewer studies have been conducted on the solute–solvent interactions between chromophores and room-temperature ionic liquids [45–47].

We have shifted the attention in our research away from traditional solvents and towards solvents containing ions—

Published online: 03 June 2011

room-temperature ionic liquids (RTILs). The properties of RTILs—a novel class of molten salts that mainly comprise organic cations and inorganic anions with melting points below room temperature—are currently receiving a great deal of attention at present [48–69]. Due to their unique ingredients, their propoerties differ drastically from those of conventional organic solvents [51, 52]. Recent work in this field has focused on the dynamics of the solvation of a solvatochromic probe in an RTIL, which has been explored through experimental studies and spectroscopic measurements [53–66]. For example, Mroncelli and coworkers [65] have monitored the steady-state spectra, rotation times, and time-resolved emission spectra of the probe 4-aminophthalimide (4-AP) in the ionic liquid 1-*n*-butyl-3-methylimidazolium hexafluorophosphate ([bmim$^+$][PF$^-$]). They found that the solvation energy of 4-AP in [bmim$^+$][PF$^-$] is comparable to those of 4-AP in highly polar but aprotic solvents, and they demonstrated that [bmim$^+$][PF$^-$] possesses essentially no hydrogen bond donating ability, so no hydrogen bonds form in the 4-AP [bmim$^+$][PF$^-$] system. The solvation and rotational dynamics of coumarin 153 (C153) in a series of phosphonium ionic liquids has also been reported by Mroncelli and coworkers [66]. To investigate the influence of specific hydrogen-bonding interactions on solvation and rotational dynamics in RTILs, Paul and Samanta [46] performed spectroscopic measurements to study the behavior of C153 in an alcohol-functionalized room-temperature ionic liquid, 1-(hydroxyethyl)-3-methylimidazolium bis(trifluoromethanesulfonyl)imide, abbreviated to [OH–emim][Tf$_2$N]. The presence of the OH group in [OH–emim][Tf$_2$N] makes it a good hydrogen bond donor, and the occurrence of hydrogen-bonding interactions between the probe molecule C153 and the hydroxylated cation was confirmed by experimental measurements; furthermore, the hydrogen bonding exerts a significant influence on the overall dynamics in RTILs [46]. Cation–anion hydrogen-bonding associations in the first solvation shell can also help to reduce the ultrafast component of the dynamics [46]. Besides investigations into the dynamics of RTILs, efforts have also been directed into the study of hydrogen bonds between ionic pairs [69]. For instance, Dhumal et al. [69] provided very useful insights into the intermolecular interactions between the 1-methyl-3-imidazolium cation and acetate anion by combining theoretical analysis with experimental methods. In other words, hydrogen bonding in RTILs is the focus of much important research.

C153 is widely utilized as a solvation probe to monitor the nature of a solvent, owing to its rigid structure and the large change in dipole moment that is caused by photoexcitation [67, 68]. C153 was also employed in the investigation reported by Seth et al., who found that a nonbonding interaction formed between the cation and the anion from the optimized structure of *N*,*N*-dimethylethanolammonium formate (DAF) [45]. Moreover, they concluded that the rotational dynamics of C153 were hindered in DAF compared to the viscous flow of DAF, which is possibly due to hydrogen-bond formation for C153 in DAF [45]. Their work has played an important role in showing that hydrogen-bond formation affects the rotational dynamics of a solute, and thus affects investigations of the nature of RTILs. Significantly, their work aroused our interest in studying the hydrogen bonding that forms between solute and solvent in RTILs. To our knowledge, little theoretical work has been performed on the hydrogen bonding between solvatochromic probe molecules and solvent molecules in novel RTIL systems. To determine the precise nature of the hydrogen bonding in this novel system, further theoretical methods need to be adopted for excited-state geometry optimization and electronic transition calculations. TDDFT is accepted as a reliable method for excited-state computation, and it can also be used to calculate the IR spectrum in the electronically excited state [70–74]. Infrared spectra also reflect hydrogen-bonding dynamics, since such dynamics occur on an ultrafast timescale that is primarily dictated by the vibrational modes of the atoms engaged in the formation of the hydrogen bond [75–78]. Therefore, in this study, we were motivated to research the hydrogen-bonded dimer C153–DAF$^+$ that forms between isolated C153 and the DAF$^+$ cation in ionic liquid DAF, and the TDDFT method was performed to study the hydrogen dynamics of this hydrogen-bonded C153–DAF$^+$ complex in the electronically excited state. The calculated absorption peak of C153 in DAF is 407 nm, which is in good agreement with experiment results [45]. At the same time, the basis set superposition error (BSSE) for the intermolecular hydrogen bond calculated using the MP2 method only accounts for a small proportion of the intermolecular hydrogen-bond binding energy. Furthermore, the calculated results for the proposed hydrogen-bonded complex C153–DAF$^+$ are also consistent with the mechanism of hydrogen bond strengthening in the electronically excited state that was first demonstrated by Zhao and Han [4].

Computational details

All of the electronic structure calculations were carried out using the TURBOMOLE program suite. The ground-state geometric optimization was performed using the density function theory (DFT) method with Becke's three-parameter hybrid exchange function and the Lee–Yang–Parr gradient-correlation functional (B3LYP functional) [79]. The excited state electronic structures were calculated

using the time-dependent density functional theory (TDDFT) with the B3LYP functional. In both the ground-state and excited-state geometric optimizations, triple-ζ valence quality basis sets with one set of polarization functions (TZVP) were chosen [80]. Fine quadrature grids 4 were also employed [81]. Harmonic vibrational frequencies in the ground state and excited state were determined by diagonalizing the Hessian [82]. The excited-state Hessian was obtained by the numerical differentiation of analytical gradients using central differences and a default displacement of 0.02 bohr. The infrared intensities were determined from the gradients of the dipole moment [83]. The BSSEs were calculated at the MP2/TZVP level.

Results and discussion

Geometric structures in the ground state

The optimized geometry in the ground state of the hydrogen-bonded complex C153–DAF$^+$, where the oxygen atom of the carbonyl group in C153 is linked to the hydrogen atom of the hydroxyl group in the cation DAF$^+$ in the RTIL DAF is shown in Fig. 1. We chose the hydrogen-bonded complex C153–DAF$^+$ here to study the ultrafast hydrogen-bonding dynamics for the following reason. As we know, in traditional polar protic solvents, the solvent molecules reorient themselves around the photoexcited solute molecules to form many solvation shells, but only the solvent molecules in the inner solvation shell can be taken into consideration early on in hydrogen-bonding dynamics that occur on the ultrafast timescale [4]. The model built by Zhao and Han for traditional polar protic solvents can be adopted for the hydrogen bonding in RTILs too, as the solvation time in most conventional solvents is extremely short (≤10 ps), but, the solvation time in neat RTILs is rather long (in the range of 0.1–10 ns) [65, 66]. In addition, only the hydrogen bond $C_1{=}O_1{\cdots}H_1{-}O_3$ joining the $C_1{=}O_1$ group of isolated C153 and the $O_3{-}H_1$ group of the isolated cation in DAF is studied here.

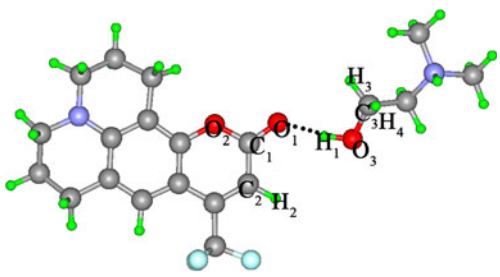

Fig. 1 Optimized geometric configuration of the hydrogen-bonded complex C153–DAF$^+$; *dotted line* denotes the intermolecular hydrogen bond

Some calculated bond lengths, angles and dihedral angles in the hydrogen-bonded complex C153–DAF$^+$ as well as the related monomers in the ground state are listed in Table 1. In the optimized geometric structure of the hydrogen-bonded complex C153–DAF$^+$, the bond angles $C_1{=}O_1{\cdots}H_1$ and $O_1{\cdots}H_1{-}O_3$ are 29.89° and 169.4°, respectively. In addition, the calculated dihedral angle $C_1{=}O_1{\cdots}H_1{-}O_3$ is 10.38°. The calculated length of the hydrogen bond $C_1{=}O_1{\cdots}H_1{-}O_3$ between the oxygen atom and hydrogen atom is 1.693 Å, which, generally speaking, is shorter than the hydrogen bonds formed in traditional solvents [4–10]. In Table 1, the calculated bond length for $C_1{=}O_1$ in isolated C153 is 1.204 Å , which increases to 1.227 Å upon the formation of the intermolecular hydrogen bond $C_1{=}O_1{\cdots}H_1{-}O_3$. At the same time, the $O_3{-}H_1$ bond in isolated cation DAF$^+$ increases slightly in length from 0.965 Å to 0.987 Å upon the formation of the intermolecular hydrogen bond $C_1{=}O_1{\cdots}H_1{-}O_3$. These changes are similar to the conditions in other traditional solvents [4–10]. The length of the $C_1{-}C_2$ bond in isolated C153 and that of the $C_3{-}O_3$ bond in the isolated cation DAF$^+$ were calculated to be 1.450 Å and 1.410 Å, respectivey, and they decrease to 1.433 Å and 1.396 Å upon the formation of the hydrogen-bonded complex C153–DAF$^+$. The $C_1{-}O_2$ bond in isolated C153 shortens from 1.391 Å to 1.366 upon the formation of the hydrogen-bonded complex C153–DAF$^+$. However, the lengths of the $C_2{-}H_2$, $C_3{-}H_3$ and $C_3{-}H_4$ bonds remain almost unchanged upon forming the hydrogen-bonded complex C153–DAF$^+$.

Electronic spectra

To understand the nature of the excited states of C153 and its hydrogen-bonded dimer C153–DAF$^+$, we need to investigate the properties of the low-lying electronically excited states in detail. The electronic excitation energies and corresponding oscillator strengths for the singlet excited states of the hydrogen-bonded dimer C153–DAF$^+$ as well as the involved monomers were calculated using the TDDFT method, and the results are shown in Table 2. Both the isolated C153 and the hydrogen-bonded complex C153–DAF$^+$ can be initially photoexcited to the S_1 state, since the S_1 states of both species have larger oscillator strengths than the other states. The absorption peak of the hydrogen-bonded complex C153–DAF$^+$ was calculated to occur at 407 nm; in experiments, the absorption maximum of C153 in DAF is found at about 425 nm [45]. Thus, our theoretical calculation is very close to the experimental value. Interestingly, it should be noted that all of the excitation energies of the hydrogen-bonded complex C153–DAF$^+$ are slightly redshifted compared with those of the isolated C153 in different electronically excited states, which indicates that the intermolecular hydrogen-bonding interactions can reduce the excitation energies of the

Table 1 Calculated bond lengths (Å), angles (°) and dihedral angles (°) of the isolated monomers and the hydrogen-bonded complex C153–DAF^+ in the ground state

Parameter		C153	DAF^+	C153–DAF^+
Bond length (Å)	C_1=O_1	1.204		1.227
	O_1···H_1			1.693
	O_3–H_1		0.965	0.987
	C_1–O_2	1.391		1.366
	C_1–C_2	1.450		1.433
	C_2–H_2	1.079		1.079
	C_3–O_3		1.410	1.396
	C_3–H_3		1.095	1.095
	C_3–H_4		1.101	1.106
Bond or dihedral angle (°)	C_1=O_1···H_1			29.89
	O_1···H_1–O_3			169.4
	C_1=O_1···H_1–O_3			10.38

hydrogen-bonded dimer C153–DAF^+. This may be useful information for us when investigating the changes in the hydrogen bond with different electronically excited states. Furthermore, the excitation energies of the isolated cation DAF^+ are much larger than those of the isolated C153 and the hydrogen-bonded dimer C153–DAF^+. The data mentioned above reveal that only the C153 moiety is electronically excited when the hydrogen-bonded complex C153–DAF^+ is photoexcited to the S_1 state; the DAF^+ moiety remains in its electronic ground state. Thus, the S_1 state of the hydrogen-bonded complex C153–DAF^+ is defined as a locally excited (LE) state [83, 84]. From Table 2, we can also obtain information on the orbital transition that contributes to the S_1 state of the isolated C153 and the hydrogen-bonded complex C153–DAF^+: both of the S_1 states correspond to the molecular orbital transition from the highest occupied orbital (HOMO) to the lowest unoccupied orbital (LUMO) according to our TDDFT calculations.

Frontier molecular orbitals

The two main frontier molecular orbitals involved in the first photoexcited state of the hydrogen-bonded complex C153–DAF^+ are depicted in Fig. 2. It is clear that the electron densities of the HOMO and LUMO orbitals are localized on the C153 moiety. Thus, the S_1 state of the hydrogen-bonded complex C153–DAF^+ has the characteristics of the LE state. After further observation, it is apparent that the electron density distribution of the HOMO is comparatively uniform, but it is deformed for the LUMO because the electron density reaches to the side of the C_1=O_1 group moiety. Consequently, the electron density of the C_1=O_1 group is strengthened in the first photoexcited state. This indicates that the electronic excitation may have a significant influence on the intensity of the hydrogen bond C_1=O_1···H_1–O_3.

Table 2 Calculated electronic excitation energies (nm) and the corresponding oscillator strengths of the isolated monomers as well as the hydrogen-bonded complex C153–DAF^+

	C153	DAF^+	C153–DAF^+
S_1	380 (0.336)	191 (0.007)	407 (0.374)
	H→L 96.3%	H→L 98.8%	H→L 95.5%
S_2	323 (0.024)	168 (0.002)	371 (0.000)
S_3	282 (0.000)	156 (0.015)	332 (0.047)
S_4	279 (0.040)	150 (0.014)	281 (0.064)
S_5	258 (0.067)	148 (0.013)	277 (0.000)
S_6	241 (0.045)	145 (0.002)	266 (0.000)

Vibrational absorption spectra

Based on the optimized excited-state geometry, all of the IR spectra of the ground state and the S_1 state for the isolated

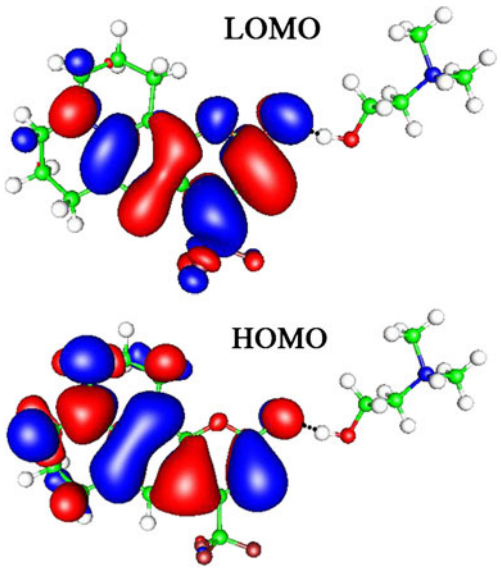

Fig. 2 Frontier molecular orbitals (MOs) of the hydrogen-bonded complex C153–DAF^+

C153 as well as the hydrogen-bonded complex C153–DAF^+ were calculated using the DFT and the TDDFT methods, respectively, and the ground-state IR spectrum of DAF^+ was also calculated for comparison.

The calculated IR spectra for both the isolated C153 and the hydrogen-bonded complex C153–DAF^+ in different electronic states over the spectra range 1000–2000 cm^{-1} are presented in Fig. 3, and the spectral regions of the C=O stretching band are indicated with red arrows. Electronic excitation from the ground state to the S_1 state of the isolated C153 induces a large redshift (of 251 cm^{-1}) in the stretching vibrational mode of the C_1=O_1 group from 1797 cm^{-1} to 1546 cm^{-1}, while the stretching vibrational mode of the C_1=O_1 group in the ground state is redshifted by only 80 cm^{-1} from 1797 cm^{-1} to 1717 cm^{-1} because of the hydrogen-bonding interactions. So, we can conclude that both the formation of the hydrogen bond C_1=O_1···H_1–O_3 and electronic excitation can cause the stretching vibrational mode of the C_1=O_1 group to redshift, whereas electronic excitation can produce a relatively large redshift in the stretching vibrational mode of the C_1=O_1 group.

The calculated IR spectra for the hydrogen-bonded complex C153–DAF^+ in different electronic states over the spectral range 2000–4000 cm^{-1} are shown in Fig. 4. Additionally, the O–H stretching band of the cation DAF^+ is presented. The stretching vibrational frequencies of the O_3–H_1 group are depicted in Fig. 4. Upon observing the stretching vibrational mode of the O_3–H_1 group, it is clear that the stretching vibrational mode of the O_3–H_1 group in the ground state is significantly redshifted (by 472 cm^{-1}) from 3812 cm^{-1} to 3340 cm^{-1} owing to the formation of the hydrogen bond C_1=O_1···H_1–O_3. This suggests that the stretching vibrational mode of the O_3–H_1 group undergoes a larger shift than that of the C_1=O_1 group upon the formation of the hydrogen bond C_1=O_1···H_1–O_3 in the ground state. As a result, the O_3–H_1 group is more sensitive

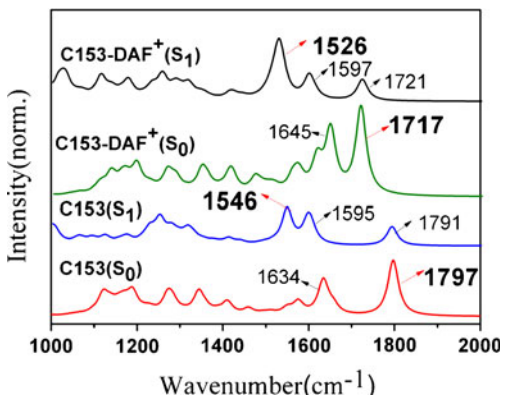

Fig. 3 Calculated IR spectra of the isolated C153 and the hydrogen-bonded complex C153–DAF^+ in different electronic states across the spectral range of the C=O stretching absorption band

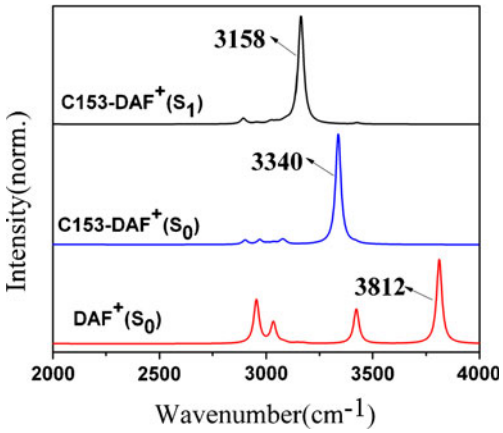

Fig. 4 Calculated O–H stretching bands of the isolated cation DAF^+ and the hydrogen-bonded complex C153–DAF^+ in different electronic states

to hydrogen-bonding interactions. As we discussed earlier, the DAF^+ moiety remains in its ground state when the hydrogen-bonded complex C153–DAF^+ is photoexcited to the S_1 state. These analyses indicate that the stretching vibrational mode of the O_3–H_1 group is an excellent mode to monitor the hydrogen-bonding dynamics of the hydrogen-bonded complex C153–DAF^+.

Comparing Fig. 3 and Fig. 4, when the hydrogen-bonded complex C153–DAF^+ is photoexcited to the S_1 state from the electronic ground state, a clear redshift in the stretching vibrational mode of the C_1=O_1 group occurs, as it changes from 1717 cm^{-1} to 1526 cm^{-1}. This suggests that the electron density of the C_1=O_1 group of the hydrogen-bonded complex C153–DAF^+ changes significantly upon electronic excitation, which is in accordance with the results we obtained in the molecular orbital (MO) analysis. At the same time, the stretching vibrational mode of the O_3–H_1 group also changes significantly, from 3340 cm^{-1} to 3158 cm^{-1}.

Excited-state hydrogen-bond strengthening

As mentioned before, when the hydrogen-bonded complex C153–DAF^+ is electronically excited to the S_1 state, the moiety of the isolated cation DAF^+ in DAF remains in the ground state. Therefore, we calculated the binding energy of the hydrogen bond in the excited state by subtracting the energy of the isolated C153 in the S_1 state and the energy of the isolated cation in the ground state from the energy of the hydrogen-bonded complex C153–DAF^+ in the S_1 state. The calculated binding energies of the hydrogen bonds as well as the corresponding hydrogen bond lengths in the ground and S_1 electronic states are shown in Table 3. Moreover, the hydrogen bond energies include BSSE corrections performed using the counterpoise method,

Table 3 Calculated bond lengths (Å), angles (°) and dihedral angles (°) for the hydrogen bond and the bonds very near to the hydrogen bond in different electronic states for isolated monomers and the hydrogen-bonded complex C153–DAF^+. Calculated hydrogen-bond binding energies E_b (kJ mol^{-1}), BSSEs (kJ mol^{-1}), and BSSE-corrected hydrogen bond binding energies E_b^{BSSE} (kJ mol^{-1}) in different electronic states are also listed

Parameter		C153–DAF^+	
		S_0	S_1
Bond length (Å)	C_1=O_1	1.227	1.242
	O_1···H_1	1.693	1.633
	O_3–H_1	0.987	0.997
	C_1–O_2	1.366	1.405
	C_1–C_2	1.433	1.417
	C_2–H_2	1.079	1.081
	C_3–O_3	1.396	1.393
	C_3–H_3	1.095	1.096
	C_3–H_4	1.106	1.107
Bond or dihedral angle (°)	C_1=O_1···H_1	128.9	123.2
	O_1···H_1–O_3	169.4	172.4
	C_1=O_1···H_1—O_3	10.38	29.28
E_b		77.19	98.46
BSSE		−7.268	−8.292
E_b^{BSSE}		69.92	90.17

$E_b^{BSSE} = E_b + BSSE$

although the BSSE corrections did not affect the binding energies notably. It is clear that the hydrogen bond C_1=O_1···H_1–O_3 is strengthened in the excited state, since the BSSE-corrected binding energy for this hydrogen bond is greatly increased by 20.25 kJ mol^{-1} from 69.92 kJ mol^{-1} in the ground state to 90.17 kJ mol^{-1} in the S_1 state. It is worth noting that the binding energies of the hydrogen bond in this novel system are quite large compared to those obtained with conventional solvents; binding energies for a hydrogen bond between a fluorescent probe and conventional solvent generally fall within the range 8–50 kJ mol^{-1} [4–6, 36–39]. Lee et al. [84] have carried out some theoretical studies on a similar system. They found that cationic and anionic dimers with short and strong hydrogen bonds (SSHBs) have larger hydrogen-bond binding energies (by almost 100 kJ mol^{-1}) than neutral hydrogen-bonded dimers, and this leads to the polarization of proton-donating H atoms on proton-accepting O/N atoms [84].

When the dimer is photoexcited, the calculated length of the C_1=O_1 bond increases from 1.227 Å to 1.242 Å, while the O_3–H_1 bond length increases to 0.997 Å from 0.987 Å. Moreover, the length of the hydrogen bond O_1···H_1 is correspondingly shortened by 0.06 Å from 1.693 Å to 1.633 Å. Thus, the conclusion that the hydrogen bond is strengthened in the photoexcited state, as seen for conventional solvents [4–10], can also be drawn for C153 hydrogen bonded to the cation DAF^+.

To show the influence of electronic excitation on the whole hydrogen-bonded complex C153–DAF^+, the changes in the lengths of the bonds adjacent to the hydrogen bond C_1=O_1···H_1–O_3 induced by electronic excitation are listed in Table 3. The C_1–O_2 bond is stretched, the C_1–C_2 bond is shortened, but the lengths of the C_2–H_2, O_3–C_3, C_3–H_3, and C_3–H_4 bonds are almost unchanged. The results basically correlate with the discussion of the LE characteristics of the S_1 state. The bond angles of C_1=O_1···H_1 and O_1···H_1–O_3 in the electronically excited state are practically the same as those in the ground state (they change by only −5.7° and 3.0° from 128.9° and 169.6°, respectively). On the other hand, the dihedral angle C_1=O_1···H_1–O_3 is significantly increased by 18.9° from 10.38° in the ground state to 29.28° in the S_1 state.

Conclusions

In this work, the electronic excited-state hydrogen-bonding dynamics of the chromophore C153 in the room-temperature ionic liquid DAF was studied using time-dependent density functional theory (TDDFT). We investigated the hydrogen bond C_1=O_1···H_1–O_3 that forms between isolated C153 and the cation DAF^+ in DAF. Based on the geometric structures and the energies of the hydrogen-bonded complex C153–DAF^+ for both the ground state and electronic excited state, it is clear that a short and strong hydrogen bond forms between C153 and the cation DAF^+ in DAF. Also, the hydrogen bond C_1=O_1···H_1–O_3 decreases from 1.693 Å to 1.633 Å, and the corresponding binding energy corrected for BSSE increases from 69.92 kJ mol^{-1} to 90.17 kJ mol^{-1}, upon photoexcitation. Using a molecular orbital analysis, we demonstrated that the S_1 state of the hydrogen-bonded complex C153–DAF^+ has the characteristics of a locally excited (LE) state, and the electron density is concentrated on the C153 moiety. The calculated maximum absorption peak of the hydrogen-bonded complex C153–DAF^+ coincides with the experimental results. In addition, we calculated the IR spectra of the ground state and the S_1 state of the hydrogen-bonded complex C153–DAF^+ as well as C153, and the ground state of the cation DAF^+ was also calculated. The vibrational absorption frequencies of the C=O group and the O–H group associated with the formation of the C_1=O_1···H_1–O_3 hydrogen bond both redshift due to photoexcitation; in other words, the hydrogen bond is strengthened when moving from the ground state to the S_1 state. Our calculations also revealed that the hydrogen bond C_1=O_1···H_1–O_3 linking the oxygen atom of the C=O group in C153 and the hydrogen atom of

the O–H group in cation DAF^+ is stronger than those formed in conventional solvents; the polarization of the cation in DAF is responsible for the strengthening of the hydrogen bond $C_1{=}O_1{\cdots}H_1{-}O_3$. More research effort should be directed into studying the hydrogen bonds formed in ionic liquids.

Acknowledgments This work was supported by the National Natural Science Foundation of China (grant nos. 21036006) and the Key Laboratory of Industrial Ecology and Environmental Engineering, China Ministry of Education.

References

1. Han KL, Zhao GJ (2010) Hydrogen bonding and transfer in the excited state. Wiley, Chichester. doi:10.1002/9780470669143. ISBN 978-0-470-66677-7
2. Banno M, Ohta K, Tominaga K (2008) Ultrafast vibrational dynamics and solvation complexes of methyl acetate in methanol studied by sub-picosecond infrared spectroscopy. J Raman Spectrosc 39:1531–1537
3. Liu S, Kokot S, Will G (2009) Photochemistry and chemometrics—an overview. J Photochem Photobiol C 10:159–172
4. Zhao GJ, Han KL (2007) Early time hydrogen-bonding dynamics of photoexcited coumarin 102 in hydrogen-donating solvents: theoretical study. J Phys Chem A 111:2469–2474
5. Zhao GJ, Han KL (2007) Novel infrared spectra for intermolecular dihydrogen bonding of the phenol-borane-trimethylamine complex in electronically excited state. J Chem Phys 127:024306
6. Zhao GJ, Han KL (2008) Time-dependent density functional theory study on hydrogen-bonded intramolecular charge-transfer excited state of 4-dimethylamino-benzonitrile in methanol. J Comput Chem 29:2010–2017
7. Zhao GJ, Han KL (2008) Effects of hydrogen bonding on tuning photochemistry: concerted hydrogen-bond strengthening and weakening. Chem Phys Chem 9:1842–1846
8. Zhao GJ, Han KL (2008) Site-specific solvation of the photoexcited protochlorophyllide a in methanol: formation of the hydrogen-bonded intermediate state induced by hydrogen-bond strengthening. Biophys J 94:38–46
9. Zhao GJ, Chen RK, Sun MT et al (2008) Photoinduced intramolecular charge transfer and S_2 fluorescence in thiophene-π-conjugated donor–acceptor systems: experimental and TDDFT studies. Chem Eur J 14:6935–6947
10. Zhao GJ, Han KL, Stang PJ (2009) Theoretical insights into hydrogen bonding and its influence on the structural and spectral properties of aquo palladium(II) complexes: cis-$[(dppp)Pd(H_2O)_2]_2^+$, cis-$[(dppp)Pd(H_2O)(OSO_2CF_3)]^+(OSO_2CF_3)^-$, and cis-$[(dppp)Pd(H_2O)_2]_2{+}(OSO_2CF_3)_2^-$. J Chem Theory Comput 5:1955–1958
11. Duan LL, Fischer A, Xu YH, Sun LC (2009) Isolated seven-coordinate Ru(IV) dimer complex with $[HOHOH]^-$ bridging ligand as an intermediate for catalytic water oxidation. J Am Chem Soc 131:10397–10399
12. Nyhlén J, Duan LL, Åkermark B, Sun LC, Privalov T (2010) Evolution of O_2 in a seven-coordinate RuIV dimer complex with a $[HOHOH]^-$ bridge: a computational study. Angew Chem Int Edn 49:1773–1777
13. Zhao GJ, Northrop BH, Stang PJ, Han KL (2010) Photophysical properties of coordination-driven self-assembled metallosupramolecular rhomboids: experimental and theoretical investigations. J Phys Chem A 114:3418–3422
14. Nagasawa Y, Yartsev AP, Tominaga K, Johnson AE, Yoshihara K (1994) Temperature dependence of ultrafast intermolecular electron transfer faster than solvation process. J Chem Phys 101:5717–5724
15. Woutersen S, Emmerichs U, Bakker HJ (1997) Femtosecond mid-IR pump-probe spectroscopy of liquid water: evidence for a two-component structure. Science 278:658–660
16. Hamm P, Lim M, Hochstrasser RM (1998) Non-Markovian dynamics of the vibrations of ions in water from femtosecond infrared three-pulse photon echoes. Phys Rev Lett 81:5326–5329
17. Sessler JL, Sationsatham M, Brown CT et al (2001) Hydrogen-bond-mediated photoinduced electron-transfer: novel dimethylaniline—anthracene ensembles formed via Watson–Crick base-pairing. J Am Chem Soc 123:3655–3660
18. Zhao GJ, Han KL (2010) pH-controlled twisted intramolecular charge transfer (TICT) excited state via changing the charge transfer direction. Phys Chem Chem Phys 12:8914–8918
19. Chan WS, Ma CS, Kwok WM, Phillips DL (2005) Time-resolved resonance Raman and density functional theory study of hydrogen-bonding effects on the triplet state of *p*-methoxyacetophenone. J Phys Chem A 109:3454–3469
20. Benniston AC, Harriman A (2006) Charge on the move: how electron-transfer dynamics depend on molecular conformation. Chem Soc Rev 35:169–179
21. Zhao GJ, Han KL (2009) Excited-state electronic structures and photochemistry of heterocyclic annulated perylenes (HAPs) materials tuned by heteroatoms: S, Se, N, O, C, Si, and B. J Phys Chem A 113:4788–4794
22. Tsumura K, Furuya K, Sakamoto A, Tasumi M (2008) Vibrational analysis of *trans*-stilbene in the excited singlet state by time-dependent density functional theory: calculations of the Raman, infrared, and fluorescence excitation spectra. J Raman Spectrosc 39:1584–1591
23. Sandanayaka ASD, Sasabe H, Takata T, Ito O (2010) Photoinduced electron transfer processes of fullerene rotaxanes containing various electron-donors. J Photochem Photobiol C 11:73–92
24. Mallick A, Das P, Chattopadhyay N (2010) Photophysics of norharmane in solution phase: from homogeneous to micro-heterogeneous environments. J Photochem Photobiol C 11:62–72
25. Kearley GJ, Fillaux F, Baron MH, Bennington S, Tomkinson J (1994) A new look at proton transfer dynamics along the hydrogen bonds in amides and peptides. Science 264:1285–1289
26. Zhao GJ, Northrop BH, Han KL, Stang PJ (2010) The effect of intermolecular hydrogen bonding on the fluorescence of a bimetallic platinum complex. J Phys Chem A 114:9007–9013
27. Shynkar VV, Klymchenko AS, Piémont E, Demchenko AP, Mély Y (2004) Dynamics of intermolecular hydrogen bonds in the excited states of 4′-dialkylamino-3-hydroxyflavones. On the pathway to an ideal fluorescent hydrogen bonding sensor. J Phys Chem A 108:8151–8159
28. Shirota H, Ushiyama H (2008) Hydrogen-bonding dynamics in aqueous solutions of amides and acids: monomer, dimer, trimer, and polymer. J Phys Chem B 112:13542–13551
29. Yun C, You J, Kim J, Huh J, Kim E (2009) Photochromic fluorescence switching from diarylethenes and its applications. J Photochem Photobiol C 10:111–129
30. Priyadarsini KI (2009) Photophysics, photochemistry and photobiology of curcumin: studies from organic solutions, bio-mimetics and living cells. J Photochem Photobiol C 10:81–95
31. Mazur K, Heisler IA, Meech SR (2010) Ultrafast dynamics and hydrogen-bond structure in aqueous solutions of model peptides. J Phys Chem B 114:10684–10691
32. Zhao GJ, Liu JY, Zhou LC, Han KL (2007) Site-selective photoinduced electron transfer from alcoholic solvents to the chromophore facilitated by hydrogen bonding: a new fluorescence quenching mechanism. J Phys Chem B 111:8940–8945

33. Karmakar R, Samanta A (2002) Steady-state and time-resolved fluorescence behavior of C153 and PRODAN in room-temperature ionic liquids. J Phys Chem A 106:6670–6675
34. Zhao GJ, Han KL (2009) Role of intramolecular and intermolecular hydrogen bonding in both singlet and triplet excited states of aminofluorenones on internal conversion, intersystem crossing, and twisted intramolecular charge transfer. J Phys Chem A 113:14329–14335
35. Zhao GJ, Han KL (2007) Ultrafast hydrogen bond strengthening of the photoexcited fluorenone in alcohols for facilitating the fluorescence quenching. J Phys Chem A 111:9218–9223
36. Liu YF, Ding JX, Shi DH, Sun JF (2008) Time-dependent density functional theory study on electronically excited states of coumarin 102 chromophore in aniline solvent: reconsideration of the electronic excited-state hydrogen-bonding dynamics. J Phys Chem A 112:6244–6248
37. Liu YF, Ding JX, Liu RQ, Shi DH, Sun JF (2009) Revisiting the electronic excited-state hydrogen bonding dynamics of coumarin chromophore in alcohols: undoubtedly strengthened not cleaved. J Photochem Photobiol A 201:203–207
38. Wei NN, Li P, Hao C, Wang R, Xiu ZL, Chen JW, Song P (2010) Time-dependent density functional theory study of the excited-state dihydrogen bond O–H···H–Si. J Photochem Photobiol A 210:77–81
39. Han KL, He GZ, Lou NQ (1996) Effect of location of energy barrier on the product alignment of reaction A+BC. J Chem Phys 105:8699–8704
40. Chu TS, Zhang Y, Han KL (2006) The time-dependent quantum wave packet approach to the electronically nonadiabatic processes in chemical reactions. Int Rev Phys Chem 25:201–205
41. Zhou LC, Zhao GJ, Liu JF, Han KL, Wu YK, Peng XJ, Sun MT (2007) The charge transfer mechanism and spectral properties of a near-infrared heptamethine cyanine dye in alcoholic and aprotic solvents. J Photochem Photobiol A 187:305–310
42. Chen RK, Zhao GJ, Yang XC et al (2008) Photoinduced intramolecular charge-transfer state in thiophene-π-conjugated donor–acceptor molecules. J Mol Struct 876:102–109
43. Chen TY, Zhang WP, Wang XQ, Zhao GJ (2009) Theoretical insight into stereodynamics of the $O(^1D)+H_2$ (v=0–3, j=0)→OH +H reaction: a quasiclassical trajectory (QCT) study. Chem Phys 365:158–163
44. Liu YH, Zhao GJ, Li GY, Han KL (2010) Fluorescence quenching phenomena facilitated by excited-state hydrogen bond strengthening for fluorenone derivatives in alcohols. J Photochem Photobiol A 209:181–185
45. Seth D, Sarkar S, Sarkar N (2008) Solvent and rotational relaxation of coumarin 153 in a protic ionic liquid dimethylethanolammonium formate. J Phys Chem B 112:2629–2636
46. Paul A, Samanta A (2007) Solute rotation and solvation dynamics in an alcohol-functionalized room temperature ionic liquid. J Phys Chem B 111:4724–4731
47. Samanta A (2006) Dynamic stokes shift and excitation wavelength dependent fluorescence of dipolar molecules in room temperature ionic liquids. J Phys Chem B 110:13704–13716
48. Endres F, Abedin SZE (2006) Air and water stable ionic liquids in physical chemistry. Phys Chem Chem Phys 8:2101–2116
49. Chiappe C, Pieraccini D (2005) Ionic liquids: solvent properties and organic reactivity. J Phys Org Chem 18:275–297
50. Welton T (1999) Room-temperature ionic liquids. solvents for synthesis and catalysis. Chem Rev 99:2071–2083
51. Jin H, Baker GA, Arzhantev S, Dong J, Maroncelli M (2007) Solvation and rotational dynamics of coumarin 153 in ionic liquids: comparisons to conventional solvents. J Phys Chem B 111:7291–7302
52. Aki SNVK, Brennecke JF, Samanta A (2001) How polar are room-temperature ionic liquids? Chem Commun 5:413–414
53. Karmakar R, Samanta A (2002) Solvation dynamics of coumarin-153 in a room-temperature ionic liquid. J Phys Chem A 106:4447–4452
54. Karmakar R, Samanta A (2003) Intramolecular excimer formation kinetics in room temperature ionic liquids. Chem Phys Lett 376:638–645
55. Karmakar R, Samanta A (2003) Dynamics of solvation of the fluorescent state of some electron donor–acceptor molecules in roomtemperature ionic liquids, $[BMIM][(CF_3SO_2)_2N]$ and $[EMIM][(CF_3SO_2)_2N]$. J Phys Chem A 107:7340–7346
56. Saha S, Mandal PK, Samanta A (2004) Solvation dynamics of Nile Red in a room temperature ionic liquid using streak camera. Phys Chem Chem Phys 6:3106–3110
57. Arzhantsev S, Ito N, Heitz M, Maroncelli M (2003) Solvation dynamics of coumarin 153 in several classes of ionic liquids: cation dependence of the ultrafast component. Chem Phys Lett 381:278–286
58. Li GY, Zhao GJ, Han KL, He GZ (2011) A TD-DFT study on the cyanide-chemosensing mechanism of 8-formyl-7-hydroxycoumarin. J Comput Chem 32:668–674
59. Lang B, Angulo G, Vauthey E (2006) Ultrafast solvation dynamics of coumarin 153 in imidazolium-based ionic liquids. J Phys Chem A 110:7028–7034
60. Chowdhury PK, Halder M, Sanders L et al (2004) Dynamic solvation in room-temperature ionic liquids. J Phys Chem B 108:10245–10255
61. Shim Y, Duan J, Choi MY, Kim HJ (2003) Solvation in molecular ionic liquids. J Chem Phys 119:6411–6414
62. Kobrak MN, Znamenskiy V (2004) Solvation dynamics of room-temperature ionic liquids: evidence for collective solvent motion on sub-picosecond timescales. Chem Phys Lett 395:127–132
63. Shim Y, Choi MY, Kim HJ (2005) A molecular dynamics computer simulation study of room-temperature ionic liquids. II. Equilibrium and nonequilibrium solvation dynamics. J Chem Phys 122:044511
64. Ingram JA, Moog RS, Ito N, Biswas R, Maroncelli M (2003) Solute rotation and solvation dynamics in a room-temperature ionic liquid. J Phys Chem B 107:5926–5932
65. Ito N, Arzhantsev S, Heitz M, Maroncelli M (2004) Solvation dynamics and rotation of coumarin 153 in alkylphosphonium ionic liquids. J Phys Chem B 108:5771–5777
66. Zhao GJ, Liu YH, Han KL, Dou YS (2008) Dynamic simulation study on ultrafast excited-state torsional dynamics of 9,9′-bianthryl (BA) in gas phase: real-time observation of novel oscillation behavior with the torsional coordinate. Chem Phys Lett 453:29–34
67. Ravi M, Soujanya T, Samanta A, Radhakrishnan TP (1995) Excited-state dipole moments of some coumarin dyes from a solvatochromic method using the solvent polarity parameter, E_T^N. J Chem Soc Faraday Trans 91:2739–2742
68. Dhumal NR, Kim HJ, Kiefer J (2009) Molecular interactions in 1-ethyl-3-methylimidazolium acetate ion pair: a density functional study. J Phys Chem A 113:10397–10404
69. Zhou LC, Liu JY, Zhao GJ, Shi Y, Peng XJ, Han KL (2007) The ultrafast dynamics of near-infrared heptamethine cyanine dye in alcoholic and aprotic solvents. Chem Phys 333:179–185
70. Han KL, He GZ (2007) Photochemistry of aryl halides: photodissociation dynamics. J Photochem Photobiol C 8:55–66
71. Chu TS, Han KL (2008) Effect of Coriolis coupling in chemical reaction dynamics. Phys Chem Chem Phys 10:2431–2441
72. Chai S, Zhao GJ, Song P, Yang SQ, Liu JY, Han KL (2009) Reconsideration of the excited-state double proton transfer (ESDPT) in 2-aminopyridine/acid systems: role of the intermolecular hydrogen bonding in excited states. Phys Chem Chem Phys 11:4385–4390

73. Li GY, Zhao GJ, Liu YH, Han KL, He GZ (2010) TD-DFT study on the sensing mechanism of a fluorescent chemosensor for fluoride: excited-state proton transfer. J Comput Chem 31:1759–1796
74. Deloncle R, Caminade AM (2010) Stimuli-responsive dendritic structures: the case of light-driven azobenzene-containing dendrimers and dendrons. J Photochem Photobiol C 11:25–45
75. Ramaswamy S, Rajaram RK, Ramakrishnan V (2003) Vibrational spectroscopic studies of L-argininium dinitrate. J Raman Spectrosc 34:50–56
76. Max JJ, Chapados C (2004) Infrared spectroscopy of acetone-water liquid mixtures. II. Molecular model. J Chem Phys 120:6625–6641
77. Molotsky T, Huppert D (2003) Site specific solvation statics and dynamics of coumarin dyes in hexane—methanol mixture. J Phys Chem A 107:2769–2780
78. Becke AD (1993) Density-functional thermochemistry. The role of exact exchange. J Chem Phys 98:5648–5652
79. Schäfer A, Huber C, Ahlrichs R (1994) Fully optimized contracted Gaussian basis sets of triple zeta valence quality for atoms Li to Kr. J Chem Phys 100:5829–5835
80. Zhao GJ, Han KL, Lei YB, Dou YS (2007) Ultrafast excited-state dynamics of tetraphenyl-ethylene studied by semiclassical simulation. J Chem Phys 127:094307
81. Ahlrichs R, Bär M, Haser M, Horn H, Kölmel C (1989) Electronic structure calculations on workstation computers: the program system turbomole. Chem Phys Lett 162:165–169
82. Halls JJM, Cornil J, Dos Santos DA et al (1999) Charge- and energy-transfer processes at polymer/polymer interfaces: a joint experimental and theoretical study. Phys Rev B 60:5721–5727
83. Lemaur V, Steel M, Beljonne D, Bréodas JL, Cornil J (2005) Photoinduced charge generation and recombination dynamics in model donor/acceptor pairs for organic solar cell applications: a full quantum-chemical treatment. J Am Chem Soc 127:6077–6086
84. Lee HM, Kumar A, Kolaski M et al (2010) Comparison of cationic, anionic and neutral hydrogen bonded dimers. Phys Chem Chem Phys 12:6278–6287